

# UC Riverside

## UC Riverside Previously Published Works

### Title

Retardation effects in the Holstein-Hubbard chain at half filling

### Permalink

<https://escholarship.org/uc/item/2hk8q6rk>

### Journal

Physical Review B, 75

### Authors

Tam, Ka-Ming  
Tsai, Shan-Wen  
Campbell, David K.  
et al.

### Publication Date

2007-04-18

### DOI

10.1103/PhysRevB.75.161103

Peer reviewed

# Retardation effects in the Holstein-Hubbard chain at half-filling

Ka-Ming Tam,<sup>1</sup> S.-W. Tsai,<sup>2</sup> D. K. Campbell,<sup>1</sup> and A. H. Castro Neto<sup>1</sup>

<sup>1</sup>*Department of Physics, Boston University, 590 Commonwealth Ave., Boston, MA 02215*

<sup>2</sup>*Department of Physics, University of California, Riverside, CA 92508*

(Dated: 6th February 2008)

The ground state phase diagram of the half-filled one-dimensional Holstein-Hubbard model contains a charge-density-wave (CDW) phase, driven by the electron-phonon (e-ph) coupling, and a spin-density-wave (SDW) phase, driven by the on-site electron-electron (e-e) repulsion. Recently, the existence of a third phase, which is metallic and lies in a finite region of parameter space between these two gapped phases, has been claimed. We study this claim using a renormalization-group method for interacting electrons that has been extended to include also e-ph couplings. Our method [1] treats e-e and e-ph interactions on an equal footing and takes retardation effects fully into account. We find a direct transition between the spin- and charge-density wave states. We study the effects of retardation, which are particularly important near the transition, and find that Umklapp processes *at finite frequencies* drive the CDW instability close to the transition. We also perform determinantal quantum Monte Carlo calculations of correlation functions to confirm our results for the phase diagram.

PACS numbers: 71.10.Fd, 71.30.+h, 71.45.Lr

The interplay between electron-electron (e-e) and electron-phonon (e-ph) interactions leads to important effects in low-dimensional materials such as molecular crystals, charge transfer solids [2], conducting polymers [3], and fullerenes [4]. In narrow band electronic materials, perhaps the simplest model capturing this interplay is the Holstein-Hubbard model (HHM), where the e-e interactions are described by a on-site repulsive Coulomb term, and the electrons are coupled to dispersionless optical phonons in localized vibrational modes [5].

In the one-dimensional HHM (1DHHM) at half-filling, early quantum Monte Carlo (QMC) calculations [6] suggested that there are only two phases: the Peierls charge-density-wave (CDW) and the Mott spin-density-wave (SDW) state. The boundary between these two phases was predicted to lie along the line in parameter space where an “effective” e-e interaction vanishes:  $U_{\text{eff}} = U - 2g_{\text{ep}}^2/\omega_0 \simeq 0$ , where  $U$  is the Hubbard on-site e-e repulsion,  $g_{\text{ep}}$  is the electron-phonon coupling, and  $\omega_0$  is the phonon frequency. More recently, several authors have proposed that a third phase might exist near  $U_{\text{eff}} \simeq 0$ : a metallic, Luttinger liquid, phase [7, 8, 9], or an off-site pairing superconducting phase [10]. Large scale QMC studies [11] have indicated that there is a metallic region with dominant superconducting (SC) pairing correlations between the CDW and SDW regions. DMRG studies [12] suggest that SC does not exist but instead that both the spin and charge gaps vanish only for  $U_{\text{eff}} \simeq 0$ , suggesting that a metallic phase (with no dominant SC correlations) may exist only exactly on the boundary between the CDW and SDW phases. This is also the conclusion of two-step renormalization-group studies [14] and Lanczos diagonalization [13]. To attempt to determine which of these scenarios is correct, we study the problem here using a recently developed extended renormalization group

approach [1].

At half-filling, Umklapp scattering creates a strong tendency to open a charge gap. From the perspective of weak-coupling approaches, it is highly non-trivial to have a finite metallic, or SC, region. If such a phase is to exist, it must be that the dynamical nature of the phonons effectively suppresses Umklapp scattering. Therefore, retardation effects must be taken into account in order to investigate this issue. For this purpose, we use a multi-scale functional renormalization-group (MFRG) method [1]. Our MFRG is an extension of the RG for interacting fermions [15] that are also coupled to bosonic modes and applies to both weak ( $\lambda \ll 1$ ) and strong ( $\lambda \gg 1$ ) electron-phonon coupling limit ( $\lambda = 2N(0)g_{\text{ep}}^2/\omega_0$ ,  $N(0)$  is the electron density of states at the Fermi level). For a spherical Fermi surface, the MFRG reproduces Eliashberg’s theory at the SC instability [1], and it has also been applied in the study of effects of phonons in ladder systems [16].

The 1DHHM is given by the Hamiltonian

$$H = -t \sum_{i,\sigma} (c_{i+1,\sigma}^\dagger c_{i,\sigma} + H.c.) + U \sum_i n_{i,\uparrow} n_{i,\downarrow} + g_{\text{ep}} \sum_{i,\sigma} (a_i^\dagger + a_i) n_{i,\sigma} + \omega_0 \sum_i a_i^\dagger a_i, \quad (1)$$

where  $c_{i,\sigma}^\dagger$  ( $c_{i,\sigma}$ ) is an electron creation (annihilation) operators at site  $i$  with spin  $\sigma$ ,  $n_{i\sigma}$  is the electron number operator,  $a_i^\dagger$  ( $a_i$ ) is a creation (annihilation) operator for an optical phonon at site  $i$ ,  $t$  is the nearest-neighbor electron hopping integral. We use units such that  $t = 1 = \hbar$ .

Using a path integral formulation and integrating out the phonon fields exactly, we find that the effective (retarded) e-e interaction becomes [1]:

$$g(\mathbf{k}_1, \mathbf{k}_2, \mathbf{k}_3, \mathbf{k}_4) = U - \frac{2g_{\text{ep}}^2 \omega_0}{[\omega_0^2 + (\omega_1 - \omega_4)^2]}, \quad (2)$$

where  $\underline{k} = (k, \omega)$ . We use a notation in which, after scattering, an incoming electron with momentum and frequency  $\underline{k}_1$  ( $\underline{k}_2$ ) goes out with  $\underline{k}_4$  ( $\underline{k}_3$ ), so that  $\underline{k}_1 + \underline{k}_2 = \underline{k}_3 + \underline{k}_4$ . In the anti-adiabatic limit, where  $\omega_0 \rightarrow \infty$ , all the electronic frequency dependences are suppressed, and the HHM maps onto the standard Hubbard model with a renormalized  $U_{\text{eff}}$ . At half-filling, its ground state is charge-gapped SDW for repulsive interactions and spin-gapped degenerate CDW/SC for attractive interactions. The transition between SDW and degenerate CDW/SC occurs when the bare coupling changes sign, that is when  $U_{\text{eff}} = 0$ .

In the MFRG approach at the one-loop level, the RG flow equations for the coupling *functions*,  $g(\underline{k}_1, \underline{k}_2, \underline{k}_3, \underline{k}_4)$  with initial conditions given by (2), are given by [1]:

$$\begin{aligned} & \frac{dg(\underline{k}_1, \underline{k}_2, \underline{k}_3)}{d\Lambda} = \\ & - \int d\underline{p} \frac{d}{d\Lambda} [G_\Lambda(\underline{p}) G_\Lambda(\underline{k})] g(\underline{k}_1, \underline{k}_2, \underline{k}) g(\underline{p}, \underline{k}, \underline{k}_3) \\ & - \int d\underline{p} \frac{d}{d\Lambda} [G_\Lambda(\underline{p}) G_\Lambda(\underline{q}_1)] g(\underline{p}, \underline{k}_2, \underline{q}_1) g(\underline{k}_1, \underline{q}_1, \underline{k}_3) \\ & - \int d\underline{p} \frac{d}{d\Lambda} [G_\Lambda(\underline{p}) G_\Lambda(\underline{q}_2)] [-2g(\underline{k}_1, \underline{p}, \underline{q}_2) g(\underline{q}_2, \underline{k}_2, \underline{k}_3) \\ & + g(\underline{p}, \underline{k}_1, \underline{q}_2) g(\underline{q}_2, \underline{k}_2, \underline{k}_3) + g(\underline{k}_1, \underline{p}, \underline{q}_2) g(\underline{k}_2, \underline{q}_2, \underline{k}_3)], \end{aligned} \quad (3)$$

where  $\underline{k} = \underline{k}_1 + \underline{k}_2 - \underline{p}$ ,  $\underline{q}_1 = \underline{p} + \underline{k}_3 - \underline{k}_1$ ,  $\underline{q}_2 = \underline{p} + \underline{k}_3 - \underline{k}_2$ ,  $\int d\underline{p} = \int d\underline{p} \sum_\omega 1/(2\pi\beta)$ , and  $G_\Lambda$  is the self-energy corrected propagator at energy cut-off  $\Lambda$ . Since the interaction vertices are frequency dependent, there are also self-energy corrections. At the one-loop level, the self-energy MFRG equation is:

$$\frac{d\Sigma(\underline{k})}{d\Lambda} = - \int d\underline{p} \frac{d}{d\Lambda} [G_\Lambda(\underline{p})] [2g(\underline{p}, \underline{k}, \underline{k}) - g(\underline{k}, \underline{p}, \underline{k})]. \quad (4)$$

We have solved the coupled integral-differential equations, (3) and (4), numerically with two Fermi points ( $N_k = 2$ ) and by dividing the frequency axis into fifteen segments ( $N_\omega = 15$ ). Fig. 1 shows the discretization scheme for  $N_k = 2$  and  $N_\omega = 15$ .

We next calculate within our MFRG approach the RG flow of susceptibilities in the static (zero frequency) and long-wavelength limit. In particular, the SC susceptibility is given by:  $\chi_\Lambda^{\text{SC}}(0, 0) = \int D(1, 2) \langle c_{p_1, \uparrow} c_{-p_1, \uparrow} c_{-p_2, \uparrow}^\dagger c_{p_2, \downarrow}^\dagger \rangle$ ; and the SDW and CDW susceptibilities can be written as:  $\chi_\Lambda^\delta(\pi, 0) = \int D(1, 2) \langle c_{p_1, \sigma_1}^\dagger c_{p_1+\pi, \sigma_1} c_{p_2+\pi, \sigma_2}^\dagger c_{p_2, \sigma_2} \rangle$ , where  $p_i$  is the momentum at energy  $\xi_i$ ,  $\int D(1, 2) \equiv \int_{|\xi_1| > \Lambda} d\xi_1 J(\xi_1) \int_{|\xi_2| > \Lambda} d\xi_2 J(\xi_2) \sum_{\sigma_1, \sigma_2} s_{\sigma_1} s_{\sigma_2}$ , and  $J(\xi)$  is the Jacobian for the coordinate transformation from  $k$  to  $\xi_k$ . For  $\delta = \text{SDW}$ :  $s_\uparrow = 1, s_\downarrow = -1$ , and for  $\delta = \text{CDW}$ :  $s_\uparrow = 1, s_\downarrow = 1$ . The dominant instability is determined by the most divergent susceptibility as the cut-off  $\Lambda$  is lowered. The RG flow for the SC susceptibility is given by:

$$\frac{d\chi_\Lambda^{\text{SC}}(0, 0)}{d\Lambda} = \int d\underline{p} \frac{d}{d\Lambda} [G_\Lambda(\underline{p}) G_\Lambda(-\underline{p})] (Z_\Lambda^{\text{SC}}(\underline{p}))^2, \quad (5)$$

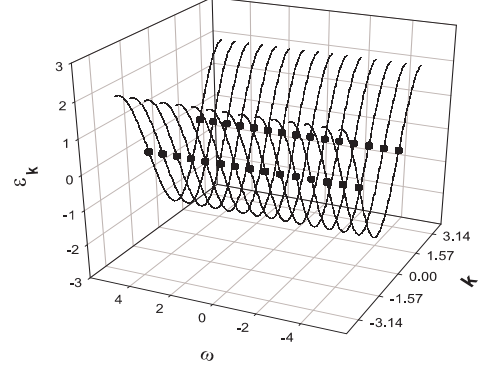


Figure 1: Discretization of the momenta in the Brillouin zone and frequencies in the frequencies axis. This figure shows the case  $N_k = 2, N_\omega = 15$ .

$$\frac{dZ_\Lambda^{\text{SC}}(\underline{p})}{d\Lambda} = - \int d\underline{p}' \frac{d}{d\Lambda} [G_\Lambda(\underline{p}') G_\Lambda(-\underline{p}')] Z_\Lambda^{\text{SC}}(\underline{p}') g^{\text{SC}}(\underline{p}', \underline{p}), \quad (6)$$

where  $g^{\text{SC}}(\underline{p}', \underline{p}) = g(\underline{p}', -\underline{p}', -\underline{p})$ , and MFRG flows for the SDW and CDW susceptibilities are,

$$\frac{d\chi_\Lambda^\delta(\pi, 0)}{d\Lambda} = - \int d\underline{p} \frac{d}{d\Lambda} [G_\Lambda(\underline{p}) G_\Lambda(\underline{p} + \underline{Q})] (Z_\Lambda^\delta(\underline{p}))^2, \quad (7)$$

$$\frac{dZ_\Lambda^\delta(\underline{p})}{d\Lambda} = \int d\underline{p}' \frac{d}{d\Lambda} [G_\Lambda(\underline{p}') G_\Lambda(\underline{p}' + \underline{Q})] Z_\Lambda^\delta(\underline{p}') g^\delta(\underline{p}', \underline{p}), \quad (8)$$

where  $\underline{Q} = (\pi, 0)$ . For  $\delta = \text{SDW}$ :  $g^\delta(\underline{p}', \underline{p}) = -g(\underline{p}' + \underline{Q}, \underline{p}', \underline{p})$ , and for  $\delta = \text{CDW}$ :  $g^\delta(\underline{p}', \underline{p}) = 2g(\underline{p}', \underline{p} + \underline{Q}, \underline{p}) - g(\underline{p} + \underline{Q}, \underline{p}', \underline{p})$ . The function  $Z^\delta(\underline{p})$  is the effective vertex in the definition of the susceptibility  $\chi^\delta$ . Its initial RG value is 1. The MFRG equations for susceptibilities are solved with initial condition  $\chi_{\Lambda=\Lambda_0}^\delta = 0$ .

In g-ology [17, 18, 19] there are only four couplings, corresponding to forward ( $g_2, g_4$ ), backward ( $g_1$ ), and Umklapp ( $g_3$ ), scattering. The charge and the spin parts are governed by  $g_3$  and  $g_1$ , respectively. Under the MFRG, each one of these couplings carries frequency dependence,  $g_i(\omega_1, \omega_2, \omega_3)$ . In the weak e-ph coupling limit ( $\lambda \ll 1$ ), the two-step RG is a good approximation, and the couplings are separated into two types: high frequency transfer,  $|\omega_1 - \omega_4| > \omega_0$ , and low frequency transfer,  $|\omega_1 - \omega_4| < \omega_0$ . However, our MFRG analysis reveals that the couplings develop additional non-trivial frequency dependence, particularly when the e-ph coupling is comparable to the e-e coupling and  $U_{\text{eff}} \approx 0$ . As we shall see, understanding this frequency structure is critical to resolving the current controversy about the behavior in the region near the CDW-SDW transition.

Deep inside the CDW and SDW regions, we fix  $\omega_0 = 1.0$  and  $U = 0.5$ , and show results of the RG flows for the susceptibilities and couplings for different values of  $g_{\text{ep}}$ . For small e-ph coupling ( $g_{\text{ep}} = 0.2$ , and  $U_{\text{eff}} > 0$ ), the SDW susceptibility exhibits a strong divergence, while

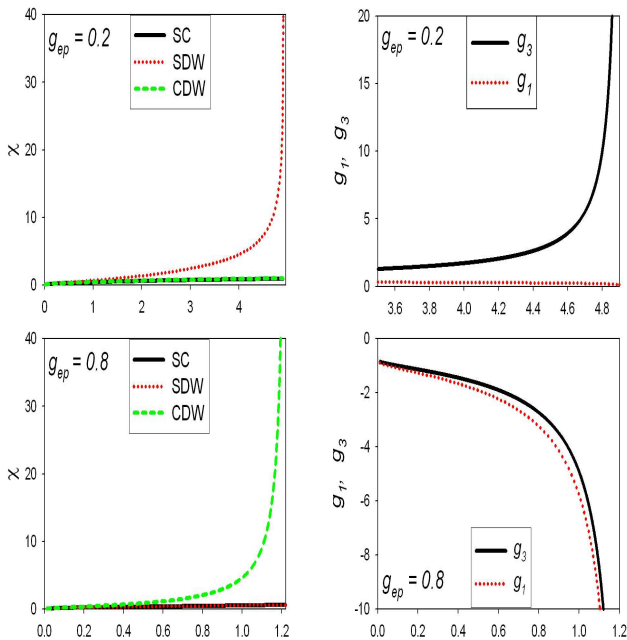


Figure 2: Left: flows of SC, SDW, and CDW susceptibilities for  $U = 0.5$  and  $\omega_0 = 1.0$ . Right: flows of Umklapp  $g_3$  and back-scattering  $g_1$ , at zero frequencies. Top:  $g_{ep} = 0.2$  ( $U_{\text{eff}} > 0$ ). Bottom:  $g_{ep} = 0.8$  ( $U_{\text{eff}} < 0$ ).

both CDW and SC susceptibilities are suppressed (Fig. 2, top). This is expected, since the on-site repulsion dominates over the retarded attractive interaction mediated by the phonons. A charge gap develops, with no spin gap, which can be inferred from the flow of the couplings: Umklapp ( $g_3$ ) diverges, whereas back-scattering ( $g_1$ ) does not. For large e-ph coupling ( $g_{ep} = 0.8$ , and  $U_{\text{eff}} < 0$ ), the CDW susceptibility diverges (Fig. 2, bottom). Now there are both spin and charge gaps, and, correspondingly, both Umklapp ( $g_3$ ) and back-scattering ( $g_1$ ) are divergent.

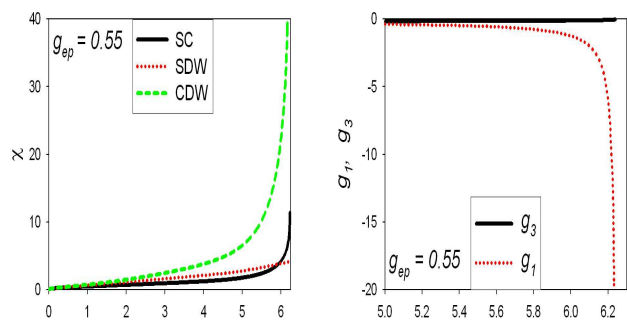


Figure 3: Left: flow of susceptibilities for  $U = 0.5$ ,  $\omega_0 = 1.0$ ,  $g_{ep} = 0.55$  ( $U_{\text{eff}} < 0$ ). Right: flows of the Umklapp scattering  $g_3$  and back-scattering  $g_1$  at zero frequency.

We next consider the region close to the CDW-SDW transition where  $U_{\text{eff}} \simeq 0$ . For  $U_{\text{eff}}$  slightly below zero ( $g_{ep} = 0.48$ ), the behavior of susceptibilities and cou-

plings is qualitatively the same as in the rest of the SDW phase (Fig. 2, top). The only difference is that the gap decreases and eventually goes to zero at the transition. Fig. 3 shows the flows for  $g_{ep} = 0.55$  ( $U_{\text{eff}}$  slightly above zero). The SC susceptibility becomes enhanced, but the CDW susceptibility still dominates. Interestingly,  $g_1(0, 0, 0)$  diverges but  $g_3(0, 0, 0)$  does not. In 1D problems without retardation, the usual interpretation is that the CDW instability occurs when  $g_1 \rightarrow -\infty$  and  $g_3 \rightarrow -\infty$  [17, 19, 20]. In the present case, since  $g_3(0, 0, 0) \rightarrow 0$ , we need to look at the frequency dependence of the couplings in order to understand what is driving the CDW instability.

In the MFRG approach, we obtain the RG flow of all the  $g_i(\omega_1, \omega_2, \omega_3)$  couplings and self-energies, and therefore can analyze how this frequency dependence evolves with the RG flow. Consider first the cases deep in the SDW and CDW phases. Fig. 4 shows contour plots of  $g_3(\omega_1, \omega_2, \omega_2, \omega_1)$  which corresponds to an Umklapp process with zero-frequency transfer,  $|\omega_1 - \omega_4| = 0$ . We plot the value of the coupling at an RG scale  $\ell$  right before the critical scale  $\ell_c$  when the instability occurs. For the SDW phase (Fig. 4, left), the existence of a charge gap is signaled by divergence in the Umklapp channel, and the most divergent  $g_3$  couplings are the ones close to zero frequency. Deep inside the CDW phase,  $g_3(0, 0, 0, 0)$  also diverges, as we have seen before from Fig. 2. However, the most divergent couplings are for large values of  $\omega_1$  and  $\omega_2$  (see Fig. 4).

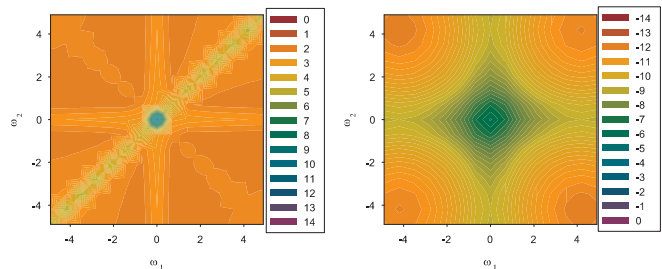


Figure 4: Plots of the Umklapp scattering  $g_3(\omega_1, \omega_2, \omega_2, \omega_1)$  for  $U = 0.5$ , and  $\omega_0 = 1.0$ . Left:  $g_{ep} = 0.2$ . Right:  $g_{ep} = 0.8$ .

The situation for  $g_{ep} = 0.55$ , shown in Fig. 5, is more intriguing. Umklapp scattering is renormalized to large values in most part of the frequency space. However, for frequencies near zero Umklapp scattering flows to very small values. From the RG flow of the susceptibilities (Figs. 2 and 3), it is clear that there is CDW instability for  $U_{\text{eff}} > 0$  and a direct transition of  $g_3$  we conclude that close to the transition to the SDW, the CDW instability is being driven by Umklapp processes *at high frequencies*. These are processes at small frequency *transfer*,  $|\omega_1 - \omega_4| \sim 0 < \omega_0$  but that nevertheless involve electrons with high frequencies ( $\omega_1$  and  $\omega_2$ ). In a two-step RG analysis, the couplings  $g_3(\omega_1, \omega_2, \omega_2, \omega_1)$ , with different  $\omega_1$  and  $\omega_2$

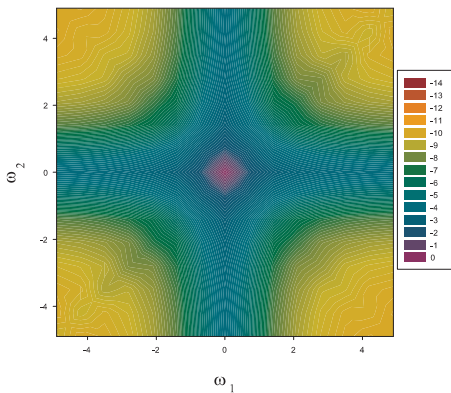


Figure 5: Plot of the Umklapp scattering  $g_3(\omega_1, \omega_2, \omega_2, \omega_1)$  for  $U = 0.5$ ,  $\omega_0 = 1.0$ , and  $g_3 = 0.55$ . Note that  $g_3(0, 0, 0)$  is flowing towards zero.

are all indistinguishable since  $|\omega_1 - \omega_4| = 0$  for all of them. Clearly, the two-step RG fails in this region.

As an independent (partial) confirmation of our MFRG results, we have also performed determinantal QMC [22] calculations for the Holstein model ( $U = 0$ ). For the charge exponent,  $K_{\text{CDW}} = \lim_{q \rightarrow 0} \pi S^\rho(q)/q$ , we obtain that  $K_{\text{CDW}} > 1$  when  $g_{\text{ep}}$  is smaller than some value that depends on  $\omega_0$ . This result agrees with that obtained in [11], using stochastic series expansion QMC [23]. For a Luttinger liquid, the scalings of ground state correlation functions are determined solely by the charge ( $K_\rho$ ) and spin ( $K_\sigma$ ) exponents. For example, in the spin-gapped regime, where  $K_\sigma = 0$ , CDW and SC correlation functions scale as  $O^{\text{CDW}}(x) \propto x^{-\alpha K_\rho} \equiv x^{-K_{\text{CDW}}}$ , and  $O^{\text{SC}}(x) \propto x^{-\beta/K_\rho} \equiv x^{-K_{\text{SC}}}$ , with  $\alpha = \beta = 1$  [17, 18, 19]. The dominant correlation is of CDW (SC) type for  $K_\rho < 1$  ( $K_\rho > 1$ ). This relation is not guaranteed to hold in the presence of phonons and retardation effects [21].

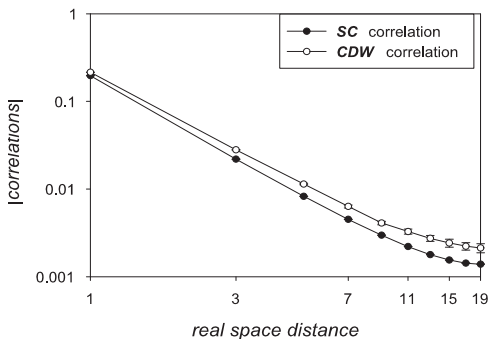


Figure 6: SC and CDW correlations for 38-sites Holstein model ( $\omega_0 = 1.0$ ,  $g_{\text{ep}} = 0.5$ ), with  $K_{\text{CDW}} = 1.032 \pm 0.005$ .

Using the determinantal QMC allows us to calculate the pairing and charge correlations directly (Fig. 6). We find that the charge correlation function decays more

slowly. This provides, at least for the case  $U = 0$ , confirmation of our MFRG results and strongly suggests that there is no region of dominant SC correlations in the half-filled 1DHMM, even though the scaling exponent of the charge correlation function can be larger than 1.

In conclusion, we have studied the ground state of 1DHMM at half-filling using the MFRG method. This technique enables us to treat retardation effects from the phonons in a systematic way. We find SDW and CDW phases, and a direct transition between them. Analysis of the frequency dependence of the  $g_3$  shows a shift in spectral weight indicating that the CDW instability near the transition is driven by dynamical Umklapp processes. Our determinantal QMC results for the charge exponent and correlation functions for the Holstein model confirm our MFRG predictions and suggest that having a charge exponent larger than one for finite size system does not mean dominant SC correlations because of breakdown of TLL relations due to retardation.

We thank Torsten Clay for instructive discussions. A.H.C.N. was supported through NSF DMR-0343790.

- 
- [1] S.-W. Tsai, A. H. Castro Neto, R. Shankar, D. K. Campbell, Phys. Rev. B **72**, 054531 (2005), Phil. Mag. 86, 2631 (2006).
  - [2] T. Ishiguro and K. Yamaji, *Organic Superconductors* (Springer-Verlag, Berlin, 1990).
  - [3] *Conjugated Conducting Polymers*, edited by H. G. Weiss (Springer-Verlag, Berlin, 1992).
  - [4] O. Gunnarsson, Rev. Mod. Phys. **69**, 575 (1997).
  - [5] T. Holstein, Ann. Phys. **8**, 325 (1959).
  - [6] J. E. Hirsch and E. Fradkin, Phys. Rev. B **27**, 4302 (1983); J. E. Hirsch, Phys. Rev. B **31**, 6022 (1985).
  - [7] C. Wu, *et al.*, Phys. Rev. B **52**, R15683 (1995).
  - [8] E. Jeckelmann, C. Zhang, and S. White, Phys. Rev. B **60**, 7950 (1999).
  - [9] Y. Takada and A. Chatterjee, Phys. Rev. B **67**, 081102 (2003).
  - [10] Y. Takada, J. Phys. Soc. Jpn. **65**, 1544 (1996).
  - [11] R. T. Clay, R. P. Hardikar, Phys. Rev. Lett. **95**, 096401 (2005).
  - [12] M. Tezuka, R. Arita, H. Aoki, Physica B **359**, 708 (2005), Phys. Rev. Lett. **95**, 226401 (2005).
  - [13] H. Feshke, *et al.*, Phys. Rev. B **69**, 165115 (2004).
  - [14] I. P. Bindloss, Phys. Rev. B **71**, 205113 (2005).
  - [15] R. Shankar, Rev. Mod. Phys. **66**, 129 (1994).
  - [16] K.-M. Tam, *et al.*, cond-mat/0603055.
  - [17] V. J. Emery, in *Highly Conducting One-Dimensional Solids*, p. 327, edited by J. T. Devreese, *et al.* (Plenum, New York, 1979).
  - [18] J. Sólyom, Adv. Phys. **28**, 201 (1979).
  - [19] J. Voit, Rep. Prog. Phys. **58**, 977 (1995).
  - [20] M. Nakamura, Phys. Rev. B **61**, 16377 (2000).
  - [21] D. Loss and T. Martin, Phys. Rev. B **50**, 12160 (1994).
  - [22] R. Blankenbecler, *et al.*, Phys. Rev. D **24**, 2278 (1981).
  - [23] O. F. Syljuasen and A. W. Sandvik, Phys. Rev. E **66**, 046701 (2002).